

PALM: Pushing Adaptive Learning Rate Mechanisms for Continual Test-Time Adaptation

Sarthak Kumar Maharana, Baoming Zhang, and Yunhui Guo

The University of Texas at Dallas, Richardson, USA
{skm200005, bzz200006, yunhui.guo}@utdallas.edu

Abstract. Real-world vision models in dynamic environments face rapid shifts in domain distributions, leading to decreased recognition performance. Continual test-time adaptation (CTTA) directly adjusts a pre-trained source discriminative model to these changing domains using test data. A highly effective CTTA method involves applying layer-wise adaptive learning rates, and selectively adapting pre-trained layers. However, it suffers from the poor estimation of domain shift and the inaccuracies arising from the pseudo-labels. In this work, we aim to overcome these limitations by identifying layers through the quantification of model prediction uncertainty without relying on pseudo-labels. We utilize the magnitude of gradients as a metric, calculated by backpropagating the KL divergence between the softmax output and a uniform distribution, to select layers for further adaptation. Subsequently, for the parameters exclusively belonging to these selected layers, with the remaining ones frozen, we evaluate their sensitivity in order to approximate the domain shift, followed by adjusting their learning rates accordingly. Overall, this approach leads to a more robust and stable optimization than prior approaches. We conduct extensive image classification experiments on CIFAR-10C, CIFAR-100C, and ImageNet-C and demonstrate the efficacy of our method against standard benchmarks and prior methods.

1 Introduction

In a real-world setting, machine-perception systems [1] function in a rapidly changing environment. In such contexts, pre-trained vision models are susceptible to performance degradation caused by potential distribution shifts. For instance, while these models may have been trained on clean images, images captured by sensors could be corrupted by various weather conditions.

In the realm of addressing domain shifts due to image corruptions, *test-time adaptation* (TTA) has been gaining a lot of traction lately [6, 44]. Here, a pre-trained source model, with no access to its training (source) data due to privacy, is adapted to unlabeled test data through online training. One strategy in TTA involves mitigating domain shifts by adjusting the source model parameters using pseudo labels and minimizing the entropy of the model predictions [44]. While this approach effectively adapts the model to a single type of corruption, it faces two constraints when continually applied across a sequence of test tasks featuring different corruptions. Firstly, there is the issue of *error accumulation*: since pseudo labels are generated for unlabeled test data, errors accumulate

over time. Secondly, *catastrophic forgetting* occurs, resulting in a long-term loss of the model’s pre-trained knowledge due to continuous adaptations and large parameter updates across tasks.

Continual test-time adaptation (CTTA) has been recently introduced to tackle these challenges. In [8, 32, 37, 44], stable optimization is achieved by updating the batch normalization (BN) parameters or re-formulating its statistics. CoTTA [45] includes full model updates, with a teacher-student network setup, to handle the above issues. To further improve the performance of CoTTA, EcoTTA [41] introduces the attachment of "meta networks", *i.e.*, a BN layer and a convolution block, to the frozen source model for efficient adaptation.

More recently, the authors in [21] demonstrated that based on the type of distributional shift of the test data, a certain subset of layers of a pre-trained model can be "surgically" or heuristically chosen to fine-tune. Inspired by this finding, *Layer-wise Auto-Weighting* (LAW) [33] was introduced recently. LAW utilizes the Fisher Information Matrix (FIM) [36] to estimate domain shifts, automatically weighting trainable parameters and adjusting their learning rates accordingly. While LAW achieves state-of-the-art results for CTTA, it still encounters two significant limitations: **1)** It presupposes that layer-wise importance can be accurately estimated via FIM with initially generated pseudo-labels. Nevertheless, it is widely recognized that pseudo-labels are inherently noisy and unreliable. **2)** Relying on directly accumulating such approximated importance from noisy labels to calculate domain shifts can lead to inaccuracies.

In this paper, we present a novel method called PALM to push the limit of adaptive learning rate methods for CTTA. Our approach begins by identifying a subset of layers that significantly contribute to the uncertainty of model predictions. Rather than relying on pseudo-labels, we determine layer-wise importance by leveraging information from the gradient space, specifically by calculating the KL divergence between the model output and a uniform distribution. This approach eliminates dependence on pseudo-labels and enables a more accurate estimation of layer-wise importance. Subsequently, the learning rates of the parameters of these layers are adjusted based on the degree of domain shift observed in the test data. We utilize parameter sensitivity as an indicator of the degree of distribution shift and employ weighted moving averages to aggregate sensitivity from previous data batches. Compared to existing adaptive learning rate methods, our proposed approach offers a better estimation of domain shift for adjusting learning rates.

To summarise, our contributions are as follows:

- We present PALM, a novel approach to continual test-time adaptation. Specifically, we demonstrate improved schemes for adaptive learning rate methods for CTTA.
- Considering the prediction uncertainty of the model at test-time, we design an approach to automatically select layers that would require further adaptation and push the learning rates of parameters of these layers for model updates, by estimating the domain shift based on parameter sensitivity.

- Our method delivers promising results in both continual and gradual TTA across three standard benchmark datasets. In addition, we conduct and demonstrate ablation experiments on the different components of our work.

2 Related Works

Test-time adaptation (TTA): The overarching target of TTA is to adapt source models to unlabelled test data in real-time in a source-free online training fashion [16, 42, 44]. TENT [44] optimizes the Batch Normalisation (BN) parameters by minimizing the Shannon entropy [40] of the pseudo labels. In [37], the statistics of the BN parameters are replaced by the ones of the input corrupted data. Adacontrast [3] combines contrastive learning and utilizes the memory module to update the entire model’s parameters. While previous TTA methods showed significant improvements, they were demonstrated for a single domain shift at a time [4, 26, 37, 44] and did not consider continual distribution shifts.

Continual TTA (CTTA): CTTA poses an adaptation challenge wherein the model must continually adjust to evolving target data, accommodating a sequence of dynamic domain shifts. The first work, CoTTA [45], considers addressing this challenging task by setting up a teacher-student network, with full model updates. The teacher model is updated using an exponential moving average (EMA) to deal with forgetting and accumulation of errors with time. EcoTTA [41] introduces "meta networks" *i.e.* a BN layer and a convolution block are attached to the frozen source model. At every stage, an L_1 regularisation loss between the outputs of the meta network and that of the source model is computed to handle catastrophic forgetting.

Efficient fine-tuning approaches: Freezing model parameters to learn information from downstream data has witnessed a good body of work [7, 9, 22, 27, 39, 51]. Depending upon the distribution shift of the target task, in [21], the authors demonstrated that heuristically selecting a subset of convolutional blocks for training while freezing the remaining blocks works better than full fine-tuning.

Adaptive-learning rate methods: Regarding the studies on the importance of each layer in training, [47, 49] concluded that deeper layers extract task-specific features, as opposed to the shallow layers. Based on this finding, AutoLR [35] design an adapted learning rate (LR) scheme based on the weight variations between layers. Despite attempts to set different initial learning rates for each layer, these rates remain mostly constant throughout training. In the context of CTTA, LAW [33] used the FIM [36] to calculate the domain shift and automatically adjust the learning rates of parameters. However, to obtain the layer importance, the pseudo-labels are used to compute the FIM, which would be inaccurate. In addition, a direct accumulation of FIMs across domains would lead to error accumulation. Furthermore, the LR "weight" of each layer is upper-bounded by the base LR that is used, which ignores the relative "sensitivity" of parameters towards adaptation of the current batch and domain.

Parameter sensitivity: In the literature about neural network pruning, understanding the sensitivity of parameters towards training has been studied well [19, 23, 28, 29, 43]. The overall idea is that parameters with lower sensitivity

need to be adapted more with an increased learning rate, and vice-versa. [23], in addition, introduces a temporal variation of sensitivity, due to uncertainty, as another factor during the training of models for natural language understanding and machine translation tasks.

3 Background

3.1 Problem Setting

The objective of continual test-time adaptation (CTTA) is to adapt a fixed discriminative pre-trained source model, parameterized by θ_s and trained on the source dataset $(\mathcal{X}^{source}, \mathcal{Y}^{source})$, to multiple incoming tasks $\mathcal{T}_i = \{x_k\}_{k=1}^n$ where \mathcal{T}_i refers to the i^{th} task and n is the total number of batches of \mathcal{T}_i , with changes in domain distributions between tasks. At each time step, θ_s is gradually adapted to each incoming batch (x_k) of task \mathcal{T}_i in an online manner, where the model parameters are updated to θ . In this entire process of adaptation, the source dataset is unavailable for use, due to privacy and storage constraints. As evident, the source model is first parameterized by θ_s before the adaptation begins. With the continuum of tasks, at time step t , the complete model parameters θ^t consists of a matrix of parameters, given by $\theta^t = \{\theta_1^t, \theta_2^t, \dots, \theta_n^t, \dots, \theta_N^t\}$, where θ_n^t , at time t , denotes the parameters of the n^{th} trainable layer out of a total of N .

3.2 Analysis of Adaptive Learning Rate Schemes for CTTA

In this subsection, we provide a detailed view and analysis of **surgical fine-tuning** [21], **AutoLR** [35], and **LAW** [33]. This is essential to understand the design principles and reasons for having an adaptive learning rate scheme for CTTA, which also includes the motivation of our work.

To preserve the information during the source pre-training phase while fine-tuning on a target task of a different distribution, **surgical fine-tuning** [21] empirically show that heuristically fine-tuning only the first convolutional block results in a better performance over full fine-tuning. Even though it is a desirable outcome for efficient fine-tuning, in this work, we close the gap by automatically selecting the layers that would adapt well to the target task.

Inspired by [47,49], **AutoLR** [35] claims that the weight changes across layers should be in increasing order, where the weight change δw_n in the n^{th} layer with weights w_n , at epoch e , is defined as,

$$\delta w_n = \|w_n^e - w_n^{(e-1)}\| \quad (1)$$

They hypothesize that weight changes in the initial layers should be small because they extract general features whereas the deeper layers extract task-specific features. A constrained adaptive LR optimization scheme is set up to force the weight variations to increase with the layers without studying the importance of each layer during adaptation. However, the updated LR, for each layer, do not deviate too much and remain constant throughout.

As the first adaptive LR work for CTTA, **LAW** [33] hypothesizes that identifying and controlling the adaptation rate of the different layers is useful [21].

To understand the loss landscape and layer importance, the authors compute the gradient from the log-likelihood as,

$$s(\theta_n^t; x_k) = \nabla_{\theta_n^t} \log(p_{\theta^t}(x_k)) \quad (2)$$

where x_k and θ_n^t refer to the current test batch and parameters of layer n at time t . Then, the Fisher Information Matrix (FIM) [36], as a domain-shift indicator, is computed as a first-order approximation of the Hessian matrix. As it can be seen, the layer-wise importance (Eq. 2) completely relies on the pseudo-labels to compute the log-likelihood, which is highly unreliable and uncertain. Due to the distribution shift, the label quality would begin to decrease for a continuum of tasks. Furthermore, the authors propose to capture "domain-level" FIM (\hat{F}_n^t), for each layer during the adaptation, by a direct accumulation of the current layer-wise FIM (F_n^t) as,

$$\hat{F}_n^t = \hat{F}_n^{t-1} + F_n^t \quad (3)$$

Based on Eq. 3, this means that LAW [33] puts equal emphasis on \hat{F}_n^t and F_n^t , for each layer. An issue arises when F_n^t of the current batch is small but gets outweighed by a "relatively" larger \hat{F}_n^t . This raises questions on the amount of adaptation required by the n^{th} layer for batch x_k as the FIMs dynamically change for each test batch. This leads to an imbalance between the accumulated FIMs \hat{F}_n^t and the current FIM F_n^t .

Drawing from these primary observations, our method focuses on addressing the following: **1)** Based on the prediction uncertainty of the model, we automatically select a subset of layers that would require further adaptation to a task, without relying on the pseudo-labels. **2)** As an indicator of the domain shift, we leverage the idea of parameter sensitivity of these layers only and adaptively alter their learning rates. We freeze the layers that are not selected.

4 Proposed Method

In this section, we introduce and formalize our proposed method for CTTA to address the key limitations of the works discussed above. Fig. 1 diagrammatically illustrates our entire approach.

4.1 Layer Selection by Quantifying Prediction Uncertainty

CTTA maximizes model performance in the current domain and is vital to assess prediction certainty amidst domain shifts. In the literature on continual learning and TTA, several works utilize FIM [18, 33, 38]. However, the unavailability of true labels, with an unknown distribution, motivates us to capture the prediction uncertainty. Prior literature proposed methods for uncertainty from the classifier output or feature space [12, 14, 20, 24, 25]. Motivated by [15], which proposed an uncertainty scoring function from the gradient space, we compute the gradients of each layer. In essence, we backpropagate the KL divergence (KL) between the softmax probabilities and a uniform distribution $\mathbf{u} = [\frac{1}{C}, \frac{1}{C}, \dots, \frac{1}{C}] \in \mathbb{R}^C$, where C is the total number of classes. This is a measurement of how far the

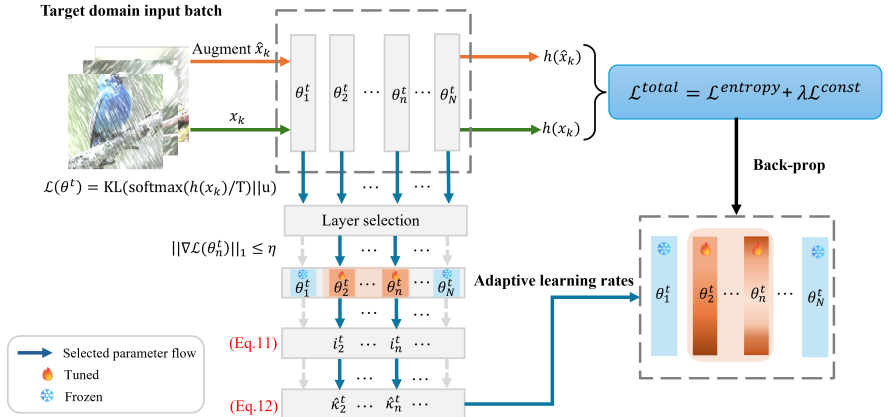


Fig. 1: PALM framework: At time t , input batch x_k is processed by the model, parameterized by θ^t . The KL-divergence between the softmax predictions and a uniform distribution is backpropagated to select the layers with the gradient norm $\leq \eta$, to quantify the uncertainty. The parameter sensitivities of these layers, as an indicator of domain shift meters, are computed to update their learning rates (Eq. 11). Finally, with the optimization objective in Eq. 16, we update the model with the adjusted learning rates of the parameters.

distribution of the model’s prediction is from a uniform distribution. Intuitively, due to the distribution shift, the KL divergence should be smaller. Let h denote the classifier of the model parameterized by θ^t . We compute the loss, denoting it as $\mathcal{L}(\theta^t)$ at time stamp t , as follows,

$$\mathcal{L}(\theta^t) = \text{KL}(\text{softmax}(\hat{h}(x_k)) || \mathbf{u}) \quad (4)$$

where $\hat{h}(x_k)$ is the classifier’s output logits ($h(x_k)$) smoothed by a temperature coefficient T *i.e.* $\hat{h}(x_k) = h(x_k)/T$. Our intuition is that batches within the same task are of the same distribution and so, smoothing the logits with large values of T will lead to them being indistinguishable. With model parameters θ^t , the gradients ($\nabla \mathcal{L}(\theta^t) = \frac{\partial \mathcal{L}(\theta^t)}{\partial \theta^t}$) can be simplified to,

$$\nabla \mathcal{L}(\theta^t) = \frac{1}{C} \sum_{j=1}^C \frac{\partial \mathcal{L}_{\text{CE}}(\hat{h}(x_k), j)}{\partial \theta^t} \quad (5)$$

On the whole, the gradients boil down to the averaged cross-entropy loss between the smoothed output logits and a uniform label (Eq. 5). In test-time adaptation, since ground-truth labels are not present, the gradients are more indicative of familiarity of the model with the batch of data. For batches within the same task, that share the same distribution, the vector norm of Eq. 5 would be higher because of a higher KL divergence since the softmax predictions would be less

uniformly distributed. However, if the norm is smaller, this would mean that the softmax outputs are closer to \mathbf{u} . Our key idea is to select all the parameters of layers that have the norm of gradients to be less than or equal to a threshold η . Layers with small gradient norms would require more adaptation for the model to make a confident prediction. Since we freeze the remaining layers, this also helps to alleviate catastrophic forgetting to a large extent by preserving the prior knowledge. And so the scoring function, for each layer, is defined as,

$$\mathcal{Z}_{\theta_n} = \|\nabla \mathcal{L}(\theta_n^t)\|_1 \quad (6)$$

As mentioned earlier, $\mathcal{Z}_{\theta_n} \leq \eta$ allows the model to adaptively determine which specific layers need further adaptation. We freeze the layers with $\mathcal{Z}_{\theta_n} > \eta$ *i.e.* set their learning rate to 0. This way, in contrast to surgical fine-tuning [21], we automatically select a subset of layers for adaptation to a batch of data.

4.2 Parameter Sensitivity as an Indicator of Domain Shift

New studies have found that model parameters demonstrate levels of criticality [2, 50] across different positions. Moreover, not all parameters adapt uniformly, and removing some can lower test generalization errors [31, 34]. Inspired by this observation, we claim that parameters have different contributions during test-time adaptation. From Sec. 4.1, we adaptively select layers that are uncertain in their predictions. For parameters of these layers only, we compute their sensitivity *i.e.* an approximation of an error when it is removed.

In our work, motivated from [19, 29, 30], we compute the parameter sensitivity of a parameter θ_n^t based on the loss (Eq. 4) as follows,

$$S_n^t = \mathcal{L}(\theta^t) - \mathcal{L}(\theta^t | \theta_n^t = 0) \quad (7)$$

Precisely, S_n^t approximates the change in the loss landscape at θ^t when θ_n^t is removed. Sensitivity, computed as a "weighting factor" of model weights [23, 29, 30], determines the level of adaptation needed for model parameters.

We utilize the gradients of parameters from the selected layers, computed by Eq. 5 to compactly derive Eq. 7 from the first-order Taylor series expansion of $\mathcal{L}(\theta^t)$ as,

$$S_n^t = |\theta_n^t \nabla \mathcal{L}(\theta_n^t)| \quad (8)$$

Our rationale is as follows: parameters with low sensitivity are pushed to have higher learning rates owing to more adaptation. However, S_n^t of θ_n^t can be highly uncertain and would have a large variation. We introduce a method to capture this "domain-level" uncertainty by computing a weighted moving average of the sensitivity S_n^t . This is formulated as,

$$\hat{S}_n^t = \alpha S_n^t + (1 - \alpha) \hat{S}_n^{(t-1)} \quad (9)$$

where \hat{S}_n^t denotes the "domain-level" sensitivity and $\alpha \in [0, 1]$ is a smoothing factor. Specifically, α decides the contribution of the current sensitivity S_n^t to \hat{S}_n^t . Since CTTA happens at batch level, it is critical to achieve a good balance

between S_n^t and \hat{S}_n^t , with a slightly larger focus on S_n^t . As it can be seen, we do not directly accumulate the "domain-level" information, unlike LAW [33].

In addition, due to large distribution shifts happening because of the continuum of tasks, larger deviations of S_n^t from \hat{S}_n^t are bound to happen. To quantify these statistics, an absolute difference between \hat{S}_n^t and S_n^t can be computed as,

$$\hat{D}_n^t = |S_n^t - \hat{S}_n^t| \quad (10)$$

We emphasize that since Eq. 9 leverages sensitivity from previously computed batches and domains, \hat{D}_n^t would act as a good indicator of how uncertain S_n^t is to the previous batches and domains, for θ_n . This would take care of error accumulation too.

To automatically alter the learning rates of these parameters, the learning rate "importance" (i_n^t) is calculated as follows,

$$i_n^t = (\hat{D}_n^t)/(\hat{S}_n^t) \quad (11)$$

Then, the final learning rate to update θ_n^t would be

$$\hat{\kappa}_n^t = \kappa * i_n^t \quad (12)$$

where κ is the base fixed learning rate. The intuition behind the formulation of Eq. 11 is as follows - smaller values of \hat{S}_n^t indicate lower sensitivity and hence larger parameter updates are required via promoting the learning rate. At the same time, large uncertainties by \hat{D}_n^t would also require larger updates. To avoid any overflow/underflow, we add ϵ ($0 < \epsilon \ll 1$) to the numerator and the denominator in Eq. 11.

4.3 Optimization Objective

Though our method is robust, it is necessary to avoid miscalibrated labels. TENT [44] minimized the Shannon entropy on the output logits, defined as,

$$\mathcal{H}(\hat{y}) = - \sum_c p(y_c) \log(p(y_c)) \quad (13)$$

where $p(y_c)$ refers to the softmax probability of class c *i.e.* $p(y_c) = \text{softmax}(h(x_k))$. Following previous CTTA work [41], we use entropy minimization as the main loss objective for adaptation where Eq. 13 is minimized for samples below a certain threshold.

$$\mathcal{L}^{entropy} = \mathbb{1}_{\mathcal{H}(\hat{y}) \leq \mathcal{H}_0} \mathcal{H}(\hat{y}) \quad (14)$$

where $\mathbb{1}$ is the indicator function and \mathcal{H}_0 is a fixed threshold set to $0.4 * \ln C$, consistently following [41]. To be fair with prior works [33, 45], we use the consistency loss between the model predictions on x_k and its augmented version \hat{x}_k to regularize the model as follows,

$$\mathcal{L}^{const} = - \sum_c p(y_c) \log(p(\hat{y}_c)) \quad (15)$$

where, $\hat{y}_c = h(\hat{x}_k)$. Our overall optimization objective is as follows,

$$\mathcal{L}^{total} = \mathcal{L}^{entropy} + \lambda \mathcal{L}^{const} \quad (16)$$

where λ indicates a regularisation coefficient to balance the consistency loss. In summary, upon calculating the parameter-specific learning rates (Eq. 12), we optimize the continually fine-tuned model to minimize Eq. 16.

5 Experiments

We draw a contrast of our proposed method against other state-of-the-art works in a continual test-time adaptation (CTTA) setting. However, to have a broader study and analysis, we also report results in a gradual test-time adaptation (GTTA) setting, following [33, 45]. In the following subsections, we describe the implementation details of both the challenging adaptation settings. For additional results and analysis, please refer to the Supplementary Material.

5.1 Experimental Settings and Baselines

Datasets and tasks. Following the standard benchmarks in CTTA, set by CoTTA [45], we evaluate our proposed method on datasets - CIFAR-10C, CIFAR-100C, and ImageNet-C, based on image corruption schemes as set in [11]. Each dataset contains a set of 15 corruption styles (*e.g.* gaussian noise, shot noise, impulse noise, defocus blur) with 5 severity levels. In line with established practices outlined in [6, 45], we report the mean classification error as the evaluation metric.

CTTA implementation details. We evaluate our approach using frameworks from prior state-of-the-art methods [3, 33, 37, 41, 44, 45]. To maintain fairness regarding the usage of pre-trained vision models, we employ WideResNet-28 [48] for CIFAR-10C, ResNeXt-29 [46] for CIFAR-100C, and ResNet-50 [10] for ImageNet-C, all available on RobustBench [5]. We optimize using an Adam optimizer [17], setting base learning rates (κ) to $5e-4$ for CIFAR-10C and CIFAR-100C, and $5e-5$ for ImageNet-C. For balancing parameter sensitivities, we set α to 0.5, 0.9, and 0.5 respectively, with temperature coefficients T set to 50, 100, and 1000 respectively. We set η to 1, 0.5, and 0.3, and λ to 0.01 throughout. Batch sizes are set to 200, 200, and 64 for each dataset, following CoTTA [45], and results are reported for the highest severity level of 5 for each task.

GTTA implementation details. In the standard CTTA setup, each task receives images with the highest severity. However, in GTTA, following [33, 41, 45], for each task the severity levels are gradually changed as $\dots 3 \rightarrow 2 \rightarrow 1 \xrightarrow[\text{change}]{\text{task}}$

$1 \rightarrow 2 \rightarrow 3 \rightarrow 4 \rightarrow 5 \rightarrow 4 \rightarrow 3 \rightarrow 2 \rightarrow 1 \xrightarrow[\text{change}]{\text{task}} 1 \rightarrow 2 \rightarrow 3 \dots$ We maintain consistency with the experimental details outlined in the CTTA setting.

Baselines. We compare our work against several CTTA baselines, including *Source*, *BN Stats Adapt* [37], *TENT Continual* [44], *CoTTA* [45], *EcoTTA* [41], *Adacontrast* [3], and *LAW* [33]. In addition, we also contrast our work against surgical fine-tuning [21]. For *EcoTTA*, we report the results on CIFAR-10C and

Table 1: Mean errors (in %) on CIFAR-10C - We report the CTТА mean errors of the 15 corruptions at a severity level of 5. We report the error of a single update (online) only using WideResNet-28 [48] for all the reported baselines.

Method	Gaussian	Shot	Impulse	Defocus	Glass	Motion	Zoom	Snow	Frost	Fog	Brightness	Contrast	Elastic Transform	Pixelate	JPEG	Mean
Source	72.3	65.7	72.9	46.9	54.3	34.8	42.0	25.1	41.3	26.0	9.3	46.7	26.6	58.5	30.3	43.5
BN Stats Adapt [37]	28.1	26.1	36.3	12.8	35.3	14.2	12.1	17.3	17.4	15.3	8.4	12.6	23.8	19.7	27.3	20.4
TENT Continual [44]	24.8	20.6	28.6	14.4	31.1	16.5	14.1	19.1	18.6	18.6	12.2	20.3	25.7	20.8	24.9	20.7
CoTTA [45]	24.3	21.3	26.6	11.6	27.6	12.2	10.3	14.8	14.1	12.4	7.5	10.6	18.3	13.4	17.3	16.2
EGoTTA [41]	23.8	18.7	25.7	11.5	29.8	13.3	11.3	15.3	15.0	13.0	7.9	11.3	20.2	15.1	20.5	16.8
Adacontrast [3]	29.1	22.5	30.0	14.0	32.7	14.1	12.0	16.6	14.9	14.4	8.1	10.0	21.9	17.7	20.0	18.5
Surgical fine-tuning [21] (continual)	27.71	24.14	33.79	12.18	33.07	13.09	10.97	15.94	15.61	13.8	7.84	10.77	21.17	16.62	22.88	18.64
LAW [33]	24.71	18.91	25.56	12.96	26.78	15.09	11.8	15.17	14.78	15.89	10.13	13.89	19.41	14.74	18.35	17.21
Ours	25.89	18.1	22.71	12.38	25.3	13.18	10.79	13.5	13.15	12.21	8.53	11.85	17.98	12.02	15.47	15.54

Table 2: Mean errors (in %) on CIFAR-100C - We report the CTТА mean errors of the 15 corruptions at a severity level of 5. We report the error of a single update (online) only using ResNeXt-29 [46] for all the reported baselines.

Method	Gaussian	Shot	Impulse	Defocus	Glass	Motion	Zoom	Snow	Frost	Fog	Brightness	Contrast	Elastic Transform	Pixelate	JPEG	Mean
Source	73.0	68	39.4	29.3	54.1	30.8	28.8	39.5	45.8	50.3	29.5	55.1	37.2	74.7	41.2	46.4
BN Stats Adapt [37]	42.1	40.7	42.7	27.6	41.9	29.7	27.9	34.9	35.0	41.5	26.5	30.3	35.7	32.9	41.2	35.4
TENT Continual [44]	37.2	35.8	41.7	37.9	51.2	48.3	48.5	58.4	63.7	71.1	70.4	82.3	88.0	88.5	90.4	60.9
CoTTA [45]	40.1	37.7	39.7	26.9	38.0	27.9	26.4	32.8	31.8	40.3	24.7	26.9	32.5	28.3	33.5	32.5
Adacontrast [3]	42.3	36.8	38.6	27.7	40.1	29.1	27.5	32.9	30.7	38.2	25.9	28.3	33.9	33.3	36.2	33.4
Surgical fine-tuning [21] (continual)	40.75	36.36	37.89	25.53	39.02	27.65	25.27	32.26	30.45	37.35	23.78	26.82	32.37	27.64	37.20	32.02
LAW [33]	41.06	36.73	38.38	25.67	37.02	27.82	25.22	30.79	30.04	37.35	24.41	27.69	31.25	27.84	34.92	31.75
Ours	37.33	32.5	34.94	26.20	35.28	27.54	24.64	28.85	29.15	34.14	23.52	26.99	31.15	26.56	34.1	30.19

ImageNet-C only since they do not use ResNeXt-29 [46] for CIFAR-100C. Following the findings of surgical fine-tuning [21], we continually fine-tune only the first convolutional block of the respective models, denoted as *Surgical fine-tuning (continual)*. We have mentioned the training details in the Supplementary. For the reported results of LAW [33], we reproduce their results strictly following their official implementation ¹ with parameters as mentioned in their paper.

5.2 CTТА Classification Results

Results on CIFAR-10C and CIFAR-100C. We contrast our proposed method against several baselines including surgical fine-tuning [21]. Tables 1 and 2 report the CTТА mean classification errors across all the domains, for each of the methods. The results reveal that our method performs the best across all training setups and baselines for both datasets. In particular, we achieve large improvements of 4.86% and 5.16% for CIFAR-10C and 5.21% and 30.71% for CIFAR-100C, over *BN Stats Adapt* [3] and *TENT Continual* [44] respectively. Concerning recent work *LAW* [33] that uses an adaptive LR scheme, our method achieves an improvement of 1.67% and 1.56% on CIFAR-10C and CIFAR-100C, respectively. It’s noteworthy that *TENT Continual* initially excels in the early

¹ <https://github.com/junia3/LayerwiseTTA/tree/main>

Table 3: Mean errors (in %) on ImageNet-C - We report the CTTA mean errors of the 15 corruptions at a severity level of 5. We report the error of a single update (online) only using ResNet-50 [10] for all the reported baselines.

Method	Gaussian	Shot	Impulse	Defocus	Glass	Motion	Zoom	Snow	Frost	Fog	Brightness	Contrast	Elastic Transform	Pixelate	JPEG	Mean
Source	97.8	97.1	98.2	81.7	89.8	85.2	78.0	83.5	77.1	75.9	41.3	94.5	82.5	79.3	68.6	82.0
BN Stats Adapt [37]	85.0	83.7	85.0	84.7	84.3	73.7	61.2	66.0	68.2	52.1	34.9	82.7	55.9	51.3	59.8	68.6
TENT Continual [44]	81.6	74.6	72.7	77.6	73.8	65.5	55.3	61.6	63.0	51.7	38.2	72.1	50.8	47.4	53.3	62.6
CoTTA [45]	84.7	82.1	80.6	81.3	79.0	68.6	57.5	60.3	60.5	48.3	36.6	66.1	47.2	41.2	46.0	62.7
ECoTTA [41]	-	-	-	-	-	-	-	-	-	-	-	-	-	-	-	63.4
Adacontrast [3]	82.9	80.9	78.4	81.4	78.7	72.9	64.0	63.5	64.5	53.5	38.4	66.7	54.6	49.4	53.0	65.5
Surgical fine-tuning [21] (continual)	83.42	79.5	77.28	86.1	82.4	72.28	61.18	63.1	64.76	51.26	35.92	72.9	56.24	46.72	50.2	65.55
LAW [33]	81.86	75.04	72.12	77.42	73.22	63.96	54.6	57.92	61.06	50.1	36.36	68.66	49.08	46.22	49.12	61.12
Ours	81.06	73.32	70.88	77.00	71.88	62.34	53.94	56.7	60.76	50.36	36.26	65.96	48.08	45.28	48.0	60.12

Table 4: Mean errors (in %) on CIFAR-10C, CIFAR-100C, and ImageNet-C - We report the gradual TTA (GTTA) mean errors averaged across all the severity levels (1→2→3→4→5).

Dataset	Source	BN Stats Adapt	TENT Continual	CoTTA	Adacontrast	Surgical fine-tuning (continual)	LAW	Ours
CIFAR-10C	24.7	13.7	20.4	10.9	12.1	11.33	10.87	9.56
CIFAR-100C	33.6	29.9	74.8	26.3	33.0	25.31	27.19	26.11
ImageNet-C	58.4	48.3	46.4	38.8	66.3	41.36	40.52	38.49

tasks but experiences error accumulation over time, leading to an increase in mean error. In the study by CoTTA [45], despite achieving good performance, the approach’s reliance on full model updates renders it computationally expensive and unsuitable for deployment. *LAW* [33] uses the uncertain pseudo labels, of each batch, to calculate the domain shift approximated via the FIM computation. The minor error that is introduced for each batch begins to propagate across all the domains. In addition, the imbalance caused by the "domain-level" FIM and the current batch’s FIM, results in a higher error rate for the initial tasks. In comparison, the computation of the model prediction uncertainty to select layers is useful in our work (Eq. 4). Another interesting observation is that with a drastic reduction in the number of trainable parameters, as in *Surgical fine-tuning (continual)*, the mean errors in Table 2 is better than most CTTA benchmarks, if not the best. This affirms the findings in [21] that concentrated adaptation, for image corruptions, in the initial layers is sufficient.

Results on Imagenet-C In Table 3, we report the CTTA results on the ImageNet-C dataset, with ResNet-50 pre-trained on ImageNet. As shown, our method outperforms all the previous CTTA baselines and *Surgical fine-tuning (continual)*. We observe an improvement of 1% over *LAW* [33]. In addition, we achieve 2.31%, 5.38%, and 30.71% improvements over CoTTA [45], Adacontrast [3], and TENT [44], respectively.

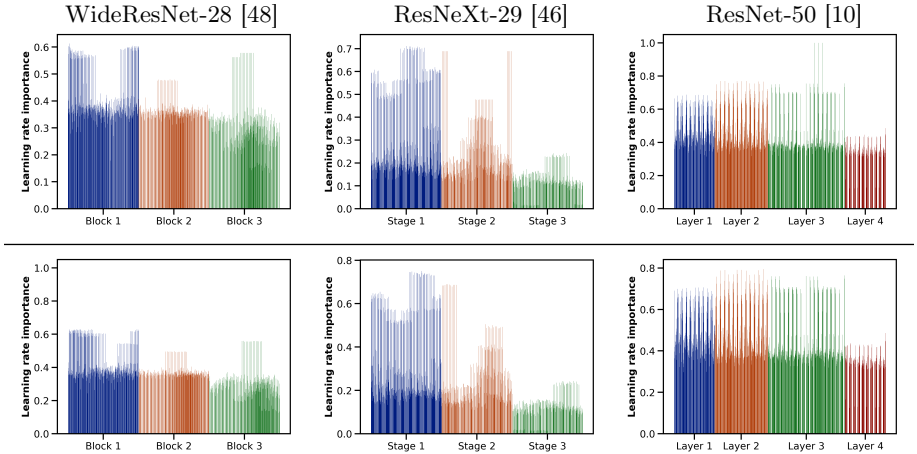


Fig. 2: Illustrations of the learning rate importances of WideResNet-28 [48], ResNeXt-29 [46], and ResNet-50 [10] during CTТА, for different convolutional blocks/stages/layers. [Top row] - Variations across respective datasets for domain `glass_blur`. [Bottom row] - Variations across respective datasets for domain `snow`.

5.3 GTТА Classification Results

Results on CIFAR-10C, CIFAR-100C, and Imagenet-C. This subsection presents the gradual test-time adaptation (GTТА) results on CIFAR-10C, CIFAR-100C, and Imagenet-C. For each task, the corruption severity of the inputs is gradually increased from levels 1 to 5, as discussed in the implementation details in Sec. 5.1. Table 4 reports the mean classification error for GTТА across all severities. We observe that, for all the datasets, our approach outperforms or performs comparably well across all the baselines [3, 33, 37, 44, 45]. With most parameters frozen during the adaptation on each batch, our method is more robust and inexpensive than CoTTA [45], which also demonstrates competitive improvements in the mean classification error.

5.4 Ablation Studies

We conduct ablation experiments to validate our approach and gain insights into its underlying mechanisms and components. Specifically, we conduct these experiments and report results on the three CTТА benchmark datasets: CIFAR-10C, CIFAR-100C, and ImageNet-100C.

Analysis of the learning rate importance. The prime objective of our work is to adaptively alter the learning rates of parameters of selected layers based on their sensitivity. In Fig. 2, we illustrate how the learning rate (LR) importance (Eq. 11) of WideResNet-28 [48], ResNeXt-29 [46], and ResNet-50 [10], averaged for a task, change during adaptation on their respective datasets. For brevity, we show two domains - `glass_blur` and `snow`. As we can see, the

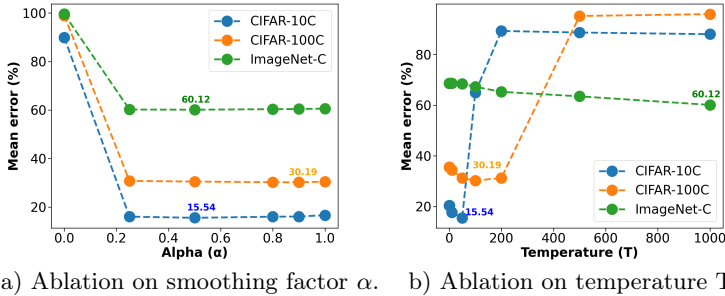


Fig. 3: Ablation results on smoothing factor α and temperature T for CIFAR-10C, CIFAR-100C, and ImageNet-C.

Table 5: Prediction uncertainty using pseudo-labels vs our method.

Dataset	Pseudo-labels	Ours
CIFAR-10C	17.98	15.54
CIFAR-100C	33.88	30.19
ImageNet-C	68.62	60.12

Table 6: Ablation results on benchmark datasets with varying λ .

λ	0	0.01	0.05	0.1	0.5	1.0
CIFAR-10C	16.84	15.54	16.45	17.03	17.65	17.93
CIFAR-100C	30.44	30.19	30.51	30.57	30.63	30.7
ImageNet-C	63.98	60.12	60.38	60.4	60.4	60.42

importance varies across domains and models. Across all the models, we notice that generally, the deeper layers have smaller associated LR importances, which means that the initial layers are adapted more to the target domain. This result completely aligns with the findings of surgical fine-tuning [21]. In addition to that, we also notice more sparsity in the deeper layers. This further confirms the necessity of freezing parameters automatically selected based on the target domain for adaptation.

Nullifying prediction uncertainty. In LAW [33], the authors make use of the pseudo-labels to automatically decide on the importance of layers for adaptation. In this, we study the effectiveness of such a design for our method *i.e.* we investigate if layer importance computed using pseudo-labels is helpful. We compute the gradients from the log-likelihood (Eq. 2) and estimate the sensitivity of the parameters of the chosen layers. Table 5 reports the mean classification errors for all the datasets. We observe that the gradients computed using the pseudo-labels are an unreliable indicator of prediction uncertainty. The scoring function (Eq. 6) computed using these gradients carries insufficient information. We achieve improvements of 2.44%, 3.69%, and 8.5% over CIFAR-10C, CIFAR-100C, and ImageNet-C, respectively.

Contribution of smoothing factor α . An important component of our method is the computation of the moving average of sensitivities across data batches, smoothed by a parameter α (Eq. 9). Fig. 3(a) illustrates the variations of the mean errors, for the benchmark datasets, for varying α . We observe that the "domain-level" sensitivity across past batches of data is indeed useful. For

$\alpha = 0$ *i.e.* when the current sensitivity of parameters of selected layers is not considered, the mean classification error for the respective datasets drastically spikes up. This suggests that the effect of the current sensitivity of selected layers is indeed required. For CIFAR-10C, we achieve the best performance when $\alpha = 0.5$ with an improvement of 1.67% over LAW [33]. Similarly, for CIFAR-100C and ImageNet-C, we see improvements of 1.56% and 1% over LAW [33], at $\alpha = 0.9$ and 0.5 respectively. With higher values of α , the results do not vary too much and are stable. Hence, attaining a balance between sensitivities from past domains (\hat{S}_n^t) and current sensitivity (S_n^t) is critical, as seen in the figure.

Logit smoothing via temperature coefficient T . In our method, we compute the KL divergence between a uniform distribution \mathbf{u} and a smoothed classifier’s output logits (Eq. 4), denoted by $\hat{h}(x_k)$. To study its influence, we choose $T \in \{0.5, 1, 10, 50, 100, 200, 1000\}$. We illustrate the results for the three datasets in Fig. 3(b). Ideally, the temperature is an indicator of the entropy of the predictions with large values pushing the distributions closer to \mathbf{u} [13]. Larger values of T spread the probability among inputs. In CTTA, since we deal with domain shifts with no labels, we argue that higher values of T are indeed useful to capture the uncertainty. With the output distribution tending towards \mathbf{u} , the KL divergence reduces (Eq. 4), indicating more uncertainty of the model and hence, adaptation. As can be seen for a difficult dataset like ImageNet-C with 1000 classes, larger values of T are useful with the error reducing as T increases. For the CIFAR datasets, $T = 50$ and 100, respectively give the best performances. However, the errors begin to rise for $T \geq 100$ which could be due to extremely large spreads of the distributions.

Robustness to the regularisation coefficient λ . As an important ablation step, we understand the effect of the parameter λ on the final optimization objective, as in Eq. 16. We set $\lambda \in \{0, 0.01, 0.05, 0.1, 0.5, 1.0\}$. We study the contributions of the consistency loss to entropy minimization. Table 6 reports the average classification errors on CIFAR-10C, CIFAR-100C, and ImageNet-C, with varying λ . For $\lambda = 0.01$, we achieve the best results across all the datasets. In addition, we observe that our method is very robust to λ *i.e.* with subtle variations to differing λ , across the datasets. In particular, for CIFAR-10C, with $\lambda = 0$ *i.e.* with no consistency loss, we achieve improvements of 0.37% and 3.86% over LAW [33] and TENT Continual [44]. For CIFAR-100C, with no consistency loss ($\lambda = 0$), we notice improvements of 1.31%, 2.06%, 4.96%, and 30.46% over LAW [33], CoTTA [45], BN Stats Adapt [37] and TENT Continual [44]. As for ImageNet-C, the consistent best setting of $\lambda = 0.01$ is better than LAW [33] by 1% and by 5.38% over Adacontrast [3]. However, with $\lambda = 0$ *i.e.* no consistency loss, we see a spike in the error rate by about 3.86% over the best setting ($\lambda = 0.01$).

6 Conclusion

In this paper, we propose a novel approach called PALM, to continual test-time adaptation. Our approach automatically decides on the importance of a layer by leveraging information from the gradient space *i.e.* by backpropagating the KL

divergence between a uniform distribution and the softmax outputs. This effectively eliminates the need for pseudo-labels. For the parameters of these layers, selected based on the norm of the gradients, the learning rates are adjusted based on their sensitivity to domain shift. Extensive experiments are conducted on benchmark datasets to demonstrate the efficacy of our method against different baselines. The results reveal that PALM achieves superior performance and pushes the state-of-the-art on several standard baselines.

References

1. Arnold, E., Al-Jarrah, O.Y., Dianati, M., Fallah, S., Oxtoby, D., Mouzakitis, A.: A survey on 3d object detection methods for autonomous driving applications. *IEEE Transactions on Intelligent Transportation Systems* **20**(10), 3782–3795 (2019)
2. Chatterji, N.S., Neyshabur, B., Sedghi, H.: The intriguing role of module criticality in the generalization of deep networks. *arXiv preprint arXiv:1912.00528* (2019)
3. Chen, D., Wang, D., Darrell, T., Ebrahimi, S.: Contrastive test-time adaptation. In: *Proceedings of the IEEE/CVF Conference on Computer Vision and Pattern Recognition*. pp. 295–305 (2022)
4. Choi, S., Yang, S., Choi, S., Yun, S.: Improving test-time adaptation via shift-agnostic weight regularization and nearest source prototypes. In: *European Conference on Computer Vision*. pp. 440–458. Springer (2022)
5. Croce, F., Andriushchenko, M., Sehwal, V., Debnedetti, E., Flammarion, N., Chiang, M., Mittal, P., Hein, M.: Robustbench: a standardized adversarial robustness benchmark. *arXiv preprint arXiv:2010.09670* (2020)
6. Döbler, M., Marsden, R.A., Yang, B.: Robust mean teacher for continual and gradual test-time adaptation. In: *Proceedings of the IEEE/CVF Conference on Computer Vision and Pattern Recognition*. pp. 7704–7714 (2023)
7. Evci, U., Dumoulin, V., Larochelle, H., Mozer, M.C.: Head2toe: Utilizing intermediate representations for better transfer learning. In: *International Conference on Machine Learning*. pp. 6009–6033. PMLR (2022)
8. Gong, T., Jeong, J., Kim, T., Kim, Y., Shin, J., Lee, S.J.: Robust continual test-time adaptation: Instance-aware bn and prediction-balanced memory. *arXiv preprint arXiv:2208.05117* (2022)
9. Guo, Y., Shi, H., Kumar, A., Grauman, K., Rosing, T., Feris, R.: Spottune: transfer learning through adaptive fine-tuning. In: *Proceedings of the IEEE/CVF conference on computer vision and pattern recognition*. pp. 4805–4814 (2019)
10. He, K., Zhang, X., Ren, S., Sun, J.: Deep residual learning for image recognition. In: *Proceedings of the IEEE conference on computer vision and pattern recognition*. pp. 770–778 (2016)
11. Hendrycks, D., Dietterich, T.: Benchmarking neural network robustness to common corruptions and perturbations. *arXiv preprint arXiv:1903.12261* (2019)
12. Hendrycks, D., Gimpel, K.: A baseline for detecting misclassified and out-of-distribution examples in neural networks. *arXiv preprint arXiv:1610.02136* (2016)
13. Hinton, G., Vinyals, O., Dean, J.: Distilling the knowledge in a neural network. *arXiv preprint arXiv:1503.02531* (2015)
14. Hsu, Y.C., Shen, Y., Jin, H., Kira, Z.: Generalized odin: Detecting out-of-distribution image without learning from out-of-distribution data. In: *Proceedings of the IEEE/CVF Conference on Computer Vision and Pattern Recognition*. pp. 10951–10960 (2020)

15. Huang, R., Geng, A., Li, Y.: On the importance of gradients for detecting distributional shifts in the wild. *Advances in Neural Information Processing Systems* **34**, 677–689 (2021)
16. Jain, V., Learned-Miller, E.: Online domain adaptation of a pre-trained cascade of classifiers. In: *CVPR 2011*. pp. 577–584. IEEE (2011)
17. Kingma, D.P., Ba, J.: Adam: A method for stochastic optimization. arXiv preprint arXiv:1412.6980 (2014)
18. Kirkpatrick, J., Pascanu, R., Rabinowitz, N., Veness, J., Desjardins, G., Rusu, A.A., Milan, K., Quan, J., Ramalho, T., Grabska-Barwinska, A., et al.: Overcoming catastrophic forgetting in neural networks. *Proceedings of the national academy of sciences* **114**(13), 3521–3526 (2017)
19. LeCun, Y., Denker, J., Solla, S.: Optimal brain damage. *Advances in neural information processing systems* **2** (1989)
20. Lee, K., Lee, K., Lee, H., Shin, J.: A simple unified framework for detecting out-of-distribution samples and adversarial attacks. *Advances in neural information processing systems* **31** (2018)
21. Lee, Y., Chen, A.S., Tajwar, F., Kumar, A., Yao, H., Liang, P., Finn, C.: Surgical fine-tuning improves adaptation to distribution shifts. arXiv preprint arXiv:2210.11466 (2022)
22. Li, X.L., Liang, P.: Prefix-tuning: Optimizing continuous prompts for generation. arXiv preprint arXiv:2101.00190 (2021)
23. Liang, C., Jiang, H., Zuo, S., He, P., Liu, X., Gao, J., Chen, W., Zhao, T.: No parameters left behind: Sensitivity guided adaptive learning rate for training large transformer models. arXiv preprint arXiv:2202.02664 (2022)
24. Liang, S., Li, Y., Srikant, R.: Enhancing the reliability of out-of-distribution image detection in neural networks. arXiv preprint arXiv:1706.02690 (2017)
25. Liu, W., Wang, X., Owens, J., Li, Y.: Energy-based out-of-distribution detection. *Advances in neural information processing systems* **33**, 21464–21475 (2020)
26. Liu, Y., Kothari, P., Van Delft, B., Bellot-Gurlet, B., Mordan, T., Alahi, A.: Ttt++: When does self-supervised test-time training fail or thrive? *Advances in Neural Information Processing Systems* **34**, 21808–21820 (2021)
27. Long, M., Zhu, H., Wang, J., Jordan, M.I.: Unsupervised domain adaptation with residual transfer networks. *Advances in neural information processing systems* **29** (2016)
28. Luo, J.H., Wu, J., Lin, W.: Thinet: A filter level pruning method for deep neural network compression. In: *Proceedings of the IEEE international conference on computer vision*. pp. 5058–5066 (2017)
29. Molchanov, P., Mallya, A., Tyree, S., Frosio, I., Kautz, J.: Importance estimation for neural network pruning. In: *Proceedings of the IEEE/CVF conference on computer vision and pattern recognition*. pp. 11264–11272 (2019)
30. Molchanov, P., Tyree, S., Karras, T., Aila, T., Kautz, J.: Pruning convolutional neural networks for resource efficient inference. arXiv preprint arXiv:1611.06440 (2016)
31. Mozer, M.C., Smolensky, P.: Skeletonization: A technique for trimming the fat from a network via relevance assessment. *Advances in neural information processing systems* **1** (1988)
32. Niu, S., Wu, J., Zhang, Y., Chen, Y., Zheng, S., Zhao, P., Tan, M.: Efficient test-time model adaptation without forgetting. In: *International conference on machine learning*. pp. 16888–16905. PMLR (2022)

33. Park, J., Kim, J., Kwon, H., Yoon, I., Sohn, K.: Layer-wise auto-weighting for non-stationary test-time adaptation. In: Proceedings of the IEEE/CVF Winter Conference on Applications of Computer Vision. pp. 1414–1423 (2024)
34. Rasmussen, C., Ghahramani, Z.: Occam’s razor. *Advances in neural information processing systems* **13** (2000)
35. Ro, Y., Choi, J.Y.: Autolr: Layer-wise pruning and auto-tuning of learning rates in fine-tuning of deep networks. In: Proceedings of the AAAI Conference on Artificial Intelligence. vol. 35, pp. 2486–2494 (2021)
36. Sagun, L., Evci, U., Guney, V.U., Dauphin, Y., Bottou, L.: Empirical analysis of the hessian of over-parametrized neural networks. arXiv preprint arXiv:1706.04454 (2017)
37. Schneider, S., Rusak, E., Eck, L., Bringmann, O., Brendel, W., Bethge, M.: Improving robustness against common corruptions by covariate shift adaptation. *Advances in neural information processing systems* **33**, 11539–11551 (2020)
38. Schwarz, J., Czarnecki, W., Luketina, J., Grabska-Barwinska, A., Teh, Y.W., Pascanu, R., Hadsell, R.: Progress & compress: A scalable framework for continual learning. In: International conference on machine learning. pp. 4528–4537. PMLR (2018)
39. Sener, O., Song, H.O., Saxena, A., Savarese, S.: Learning transferrable representations for unsupervised domain adaptation. *Advances in neural information processing systems* **29** (2016)
40. Shannon, C.E.: A mathematical theory of communication. *The Bell system technical journal* **27**(3), 379–423 (1948)
41. Song, J., Lee, J., Kweon, I.S., Choi, S.: Ecotta: Memory-efficient continual test-time adaptation via self-distilled regularization. In: Proceedings of the IEEE/CVF Conference on Computer Vision and Pattern Recognition. pp. 11920–11929 (2023)
42. Sun, Y., Wang, X., Liu, Z., Miller, J., Efros, A., Hardt, M.: Test-time training with self-supervision for generalization under distribution shifts. In: International conference on machine learning. pp. 9229–9248. PMLR (2020)
43. Theis, L., Korshunova, I., Tejani, A., Huszár, F.: Faster gaze prediction with dense networks and fisher pruning. arXiv preprint arXiv:1801.05787 (2018)
44. Wang, D., Shelhamer, E., Liu, S., Olshausen, B., Darrell, T.: Tent: Fully test-time adaptation by entropy minimization. arXiv preprint arXiv:2006.10726 (2020)
45. Wang, Q., Fink, O., Van Gool, L., Dai, D.: Continual test-time domain adaptation. In: Proceedings of the IEEE/CVF Conference on Computer Vision and Pattern Recognition. pp. 7201–7211 (2022)
46. Xie, S., Girshick, R., Dollár, P., Tu, Z., He, K.: Aggregated residual transformations for deep neural networks. In: Proceedings of the IEEE conference on computer vision and pattern recognition. pp. 1492–1500 (2017)
47. Yosinski, J., Clune, J., Bengio, Y., Lipson, H.: How transferable are features in deep neural networks? *Advances in neural information processing systems* **27** (2014)
48. Zagoruyko, S., Komodakis, N.: Wide residual networks. arXiv preprint arXiv:1605.07146 (2016)
49. Zeiler, M.D., Fergus, R.: Visualizing and understanding convolutional networks. In: Computer Vision—ECCV 2014: 13th European Conference, Zurich, Switzerland, September 6–12, 2014, Proceedings, Part I 13. pp. 818–833. Springer (2014)
50. Zhang, C., Bengio, S., Singer, Y.: Are all layers created equal? *The Journal of Machine Learning Research* **23**(1), 2930–2957 (2022)
51. Zintgraf, L., Shiarli, K., Kurin, V., Hofmann, K., Whiteson, S.: Fast context adaptation via meta-learning. In: International Conference on Machine Learning. pp. 7693–7702. PMLR (2019)

7 Supplementary Material

In this work, we propose a continual test-time adaptation method that adaptively changes the learning rates of selected parameters of the model. This involves two core steps: 1) automatically selecting a subset of layers, for further adaptation, based on the model’s prediction uncertainty. 2) as an indicator of domain shift, we utilize the sensitivity of the parameters of the selected layers, to the loss landscape, to weigh the learning rate importance. In this supplement to the main paper, we offer further elaboration and experimental findings on the following:

- We critically analyze the effectiveness of **different vector norms** on the gradients computed by backpropagating the KL divergence between the predicted probabilities and a uniform distribution in Sec. 7.1.
- We present an ablation study, in Sec. 7.2, **on the threshold that upper bounds the scoring function of gradients.**
- We study the different formulations of the **learning rate "importance"** in Sec. 7.3.
- We evaluate our proposed approach in a more realistic and extremely challenging setting *i.e.* **Mixed-Domain Test-Time Adaptation (MDTTA)** in Sec. 7.4.
- We draw a contrast between our work and **AutoLR** [35] in Sec. 7.5, an adaptive learning rate method for efficient vision model fine-tuning on downstream tasks.
- We validate our method across **various pre-trained source models** in Sec. 7.6.

7.1 Effectiveness of p-norms to Compute the Scoring Function (\mathcal{Z}_{θ_n})

Table 7: Mean errors (in %) on CIFAR-10C, CIFAR-100C, and ImageNet-C - We report the CTTA mean errors for different p-norms that are used for the scoring function.

p	0	0.5	1	2	3	4	5	∞
CIFAR-10C	20.35	16.32	15.54	86.61	83.42	82.59	82.08	81.83
CIFAR-100C	35.5	30.41	30.19	69.57	69.53	70.32	69.88	74.48
ImageNet-C	68.61	60.23	60.12	97.06	96.90	96.85	96.84	96.90

In our proposed approach, we decide upon the usage of the L_1 vector norm to bound the gradients backpropagated from the KL divergence between a uniform distribution $\mathbf{u} = [\frac{1}{C}, \frac{1}{C}, \dots, \frac{1}{C}] \in \mathbb{R}^C$, where C is the total number of classes, and the model’s softmax outputs. This helped in selecting the model layers that would require further adaptation since smaller norm values translate to the fact that the softmax outputs are closer to \mathbf{u} . In this experiment, we justify the usage

of the L_1 norm for such a computation. To be specific, we compute a variety of p-norms *i.e.* $p \in \{0, 0.5, 1, 2, 3, 4, 5, \infty\}$. Table 7 reports the mean classification errors on the benchmark datasets CIFAR-10C, CIFAR-100C, and ImageNet-C, upon varying the scoring function. Mathematically, for a vector \mathbf{r} , the p-norm is defined as:

$$\|\mathbf{r}\|_p = \left(\sum_i |r_i|^p \right)^{\frac{1}{p}} \quad (17)$$

When $p > 1$, the emphasis is on the larger components of \mathbf{r} leading to even sparser representations. In the gradient space, the scoring functions with large values of p do not get a good representation of the divergence. This can be seen from the reported results with the errors getting amplified for all the datasets. For $p < 1$, even though we do not observe large errors, they do not outperform $p = 1$ because of the emphasis on smaller components. Interestingly, with $p \rightarrow 1$, the error gap begins to close.

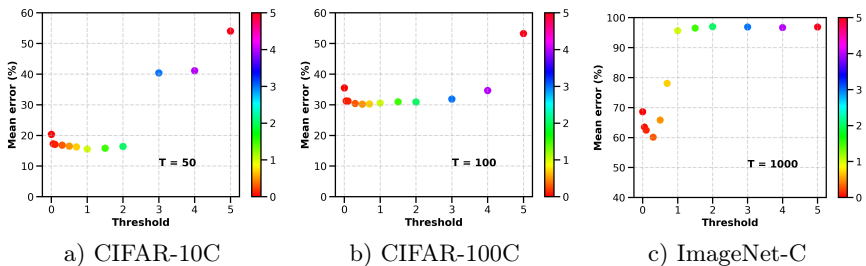


Fig. 4: Classification mean errors for different values of η . We select the subset of layers with the scoring function $\mathcal{Z}_{\theta_n} \leq \eta$ while freezing the rest by not updating them.

7.2 Ablation on η

In the previous subsection, we discussed the analysis and motivation of using an L_1 norm on the computed gradients to select the subset of layers that would require further adaptation, an automatic alternative to surgical fine-tuning [21]. In Fig. 4 we illustrate the effects of $\mathcal{Z}_{\theta_n} \leq \eta$ on the mean errors of CIFAR-10C, CIFAR-100C, and ImageNet-C. In the main paper, we argue that larger values of temperature T are required to capture the prediction uncertainty since the output distribution would largely tend towards \mathbf{u} . Since the temperature plays a large role in smoothing the logits, we report $\eta \in \{0, 0.05, 0.1, 0.3, 0.5, 0.7, 1.0, 1.5, 2, 3, 4, 5\}$. From the figure, it is apparent that smaller values of η , with their corresponding temperature T are favored, leading to not updating the majority of parameters of the subset of layers that were chosen. This reduces the computational cost while simultaneously enhancing classification performance and adaptation through our approach.

7.3 Understanding the Formulation of the Learning Rate Importance

The scale or "importance" of the learning rates of parameters in selected layers, is formulated as:

$$i_n^t = \hat{D}_n^t / \hat{S}_n^t \quad (18)$$

where \hat{D}_n^t indicates how uncertain \hat{S}_n^t is to previous batches of different domains. We increase the learning rate of less sensitive and more uncertain parameters. In this ablation, we focus on the different alternatives that Eq. 11 can take. In Table 8 we outline the different alternatives.

Table 8: Different alternatives of Eq. 11 to compute the learning rate importance for our work.

Alternative	Description
1. $\hat{D}_n^t / \hat{S}_n^t$	Proposed.
2. $\hat{D}_n^t * \hat{S}_n^t$	Increase the learning rates for highly sensitive/uncertain parameters.
3. \hat{S}_n^t	Exclude the influence of the uncertainty of \hat{S}_n^t <i>i.e.</i> \hat{D}_n^t .
4. $1/\hat{S}_n^t$	Study the influence of excluding \hat{D}_n^t .
5. \hat{D}_n^t	Study the influence of excluding \hat{S}_n^t .
6. $\hat{S}_n^t / \hat{D}_n^t$	Lower the learning rates of highly uncertain sensitive parameters.

Fig. 5 illustrates the mean errors of the datasets using the different alternatives of Eq. 11. In alternatives 2, 3, and 6, the focus is on increasing the learning rates for highly sensitive parameters *i.e.* In 4 and 5, we seek to analyze performance while specifically excluding the influence of each factor one at a time. As can be seen, for alternatives 2, 3, and 5, we see a small spike in mean error over the best (alternative 1). For alternative 6, the uncertainty captured by \hat{D}_n^t decreases the learning rate, leading to a sharp rise in errors. A similar conclusion can be drawn about alternative 4 *i.e.* the learning rates are elevated for parameters with low sensitivity. Hence, modeling the uncertainty and sensitivity of parameters is crucial with both complementing each other, as in our proposed scheme.

Table 9: We report the Mixed-Domain TTA (MDTTA) mean errors (in %) with a test batch of corruption severity 5.

Dataset	LAW	Ours
CIFAR-10C	49.94	40.96
CIFAR-100C	43.01	36.15
ImageNet-C	91.01	91.38

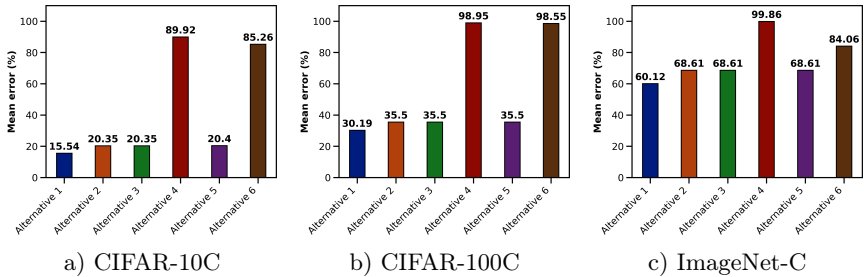


Fig. 5: Illustration of mean errors on CIFAR-10C, CIFAR-100C, and ImageNet-C based on the alternative formulations of the learning rate "importance" (Eq. 11).

7.4 Mixed-Domain Test-Time Adaptation

In the main paper, we perform and report experimental results on two test-time adaptation settings - continual and gradual. However, to challenge current approaches to a larger extent, we perform adaptation in a very "realistic" setting where consecutive batches of data could originate from different distributions. We call this as Mixed-Domain Test-Time Adaptation (MDTTA). In standard CTTA, with the idea of tasks and distributions, we adapt the model to a series of tasks where each task has batches from a single distribution. There is no awareness of when a new task arrives. However, in MDTTA, with no concept of a task, consecutive batches most likely have different image corruptions/distributions. Such a realistic TTA setting should be critically studied since in real-world scenarios, the model is never aware of how quickly the distribution changes.

Table 9 reports the MDTTA results using *LAW* [33] and our method on CIFAR-10C, CIFAR-100C, and ImageNet-C. Adaptive learning rate TTA methods like *LAW* [33] claim to capture the domain shift of a batch by computing the Fisher Information Matrix (FIM) [36], based on the pseudo-labels, to decide on the layer importance. As seen from the results, such an approach is not very useful for MDTTA. Along similar lines, our approach, which automatically decides on the required subset of layers for further adaptation based on the model's current prediction uncertainty and computes their parameter sensitivity, achieves staggering improvements of 8.98% and 6.86% over *LAW* [33] for CIFAR-10C and CIFAR-100C, respectively. On ImageNet-C, we achieve comparable performances.

7.5 Comparison with AutoLR [35]

Ro *et al.* proposed AutoLR [35], an adaptive learning rate method, for efficient fine-tuning, based on the weight variations between layers of a model. With the intended increment in weight change across layers, the authors propose a target weight change based on manually chosen hyper-parameters that decide the range of weight change. With the desired weight variation being very sensitive to the hyper-parameters, the learning rates change very little. In this subsection, we

Table 10: Fine-grained classification errors (in %) on CIFAR-10C and CIFAR-100C by AutoLR and ours.

CIFAR-10C																
Method	Gaussian	Shot	Impulse	Defocus	Glass	Motion	Zoom	Snow	Frost	Fog	Brightness	Contrast	Elastic Transform	Pixelate	JPEG	Mean
AutoLR [35]	26.98	23.9	33.54	13.23	33.26	15.84	13.58	18.59	17.29	16.64	11.51	16.08	26.37	23.02	31.72	21.44
Ours	25.89	18.1	22.71	12.38	25.3	13.18	10.79	13.5	13.15	12.21	8.53	11.85	17.98	12.02	15.47	15.54
CIFAR-100C																
AutoLR [35]	39.51	35.11	37.09	27.55	37.91	30.62	28.74	34.61	34.50	40.76	30.51	35.47	36.79	34.09	41.31	34.97
Ours	37.33	32.5	34.94	26.20	35.28	27.54	24.64	28.85	29.15	34.14	23.52	26.99	31.15	26.56	34.1	30.19

contrast our work against AutoLR [35] by adapting their work to the CTTA setting. We optimize our model using SGD with a learning rate of 1e-3 and a momentum factor of 0.9. The final optimization objective is the same as ours *i.e.* entropy minimization and consistency loss.

In Table 10, we report results for CIFAR-10C and CIFAR-100C to demonstrate the effectiveness of our work. We observe improvements of 5.9% and 4.78% over AutoLR [35] for CIFAR-10C and CIFAR-100C respectively. For CIFAR-100C, an interesting observation is that for the initial tasks, the error gap between AutoLR [35] and our approach is not too much. However, towards the later stages, the error gap rises. A plausible explanation for this is that AutoLR [35] does not consider or utilize the distributional shift between tasks to update the learning rates of layers. In our work, due to the computation of the parameter sensitivity, we approximate the amount of adaptation that is required by the batch and update its learning rate accordingly.

Table 11: Classification mean error (in %) on CIFAR-10C using different source models.

Method	WideResNet-28 [48]	ResNeXt-29 [46]	WideResNet-40 [5]	ResNet-50 [26]
Source	43.5	18.0	18.3	48.8
BN Stats Adapt [37]	20.4	13.3	14.6	16.1
TENT Continual [44]	20.7	14.8	12.5	14.8
CoTTA [45]	16.2	11.0	12.7	13.1
Adacontrast [3]	18.5	11.0	11.9	14.5
LAW [33]	17.21	10.64	11.79	12.62
Ours	15.54	9.05	11.03	11.42

7.6 CTTA Performance with Other Models

Following LAW [33], we carry out additional experiments to confirm the adaptable effectiveness of our approach. To be fair and consistent with respect to the source models, in addition to WideResNet-28 [48], we report results on ResNeXt-29 [46], WideResNet-40 from [5], and ResNet-50 from [26] for CIFAR-10C and CIFAR-100C benchmark datasets. For ImageNet-C, we use ResNeXt-50 [46],

Table 12: Classification mean error (in %) on CIFAR-100C using different source models. **Table 13:** Classification mean error (in %) on ImageNet-C using different source models.

Method	ResNeXt-29 [46]	WideResNet-40 [5]	ResNet-50 [26]
Source	46.4	46.8	73.8
BN Stats Adapt [37]	35.4	39.3	43.7
TENT Continual [44]	60.9	36.9	44.2
CoTTA [45]	32.5	38.2	37.6
Adacontrast [3]	33.4	37.1	41.3
LAW [33]	31.75	35.82	39.3
Ours	30.19	33.93	37.78

Method	ResNet-50 [10]	ResNeXt-50 [46]	WideResNet-50 [48]
Source	82.0	78.9	78.9
BN Stats Adapt [37]	68.6	67.1	66.2
TENT Continual [44]	62.6	58.7	57.7
CoTTA [45]	62.7	59.8	57.9
Adacontrast [3]	65.5	63.1	63.3
LAW [33]	61.12	57.7	56.25
Ours	60.12	56.88	54.66

WideResNet-50 [48], and ResNet-50 [10]. For each, we document the mean classification error over 5 rounds. The goal of these experiments is to eliminate any bias regarding the selection of models discussed in the main paper. Tables 11, 12, and 13 report our results against *Source*, *BN Stats Adapt* [37], *TENT Continual* [44], *CoTTA* [45], *Adacontrast* [3], and *LAW* [33] with their respective models.

In Table 11, we report the mean classification errors on the CIFAR-10C dataset for different baselines using WideResNet-28 [48], ResNeXt-29 [46], WideResNet-40 from [5], and ResNet-50 from [26]. Our method clearly outperforms all the baselines using the different source models. In particular, we obtain performance improvements of 1.67%, 1.59%, 0.76%, and 1.2% for the respective models, over LAW [33].

Similarly, Tables 12 and 13 report the mean errors on CIFAR-100C and ImageNet-C. For CIFAR-100C, we observe that *TENT Continual* [44] does not scale well with change in models *i.e.* the error increases by 24% and 16.7% for ResNeXt-29 over WideResNet-40 [5] and ResNet-50 [26]. The performance of *CoTTA* [45] with ResNet-50 [10] demonstrates remarkable comparability to the outcomes achieved by our approach. Adaptive learning rate methods, especially ours, establish a new baseline for CTTA performance across all models with mean errors. On the ImageNet-C dataset, we observe comparable performances between *TENT Continual* [44] and *CoTTA* [45]. Across all the respective models on ImageNet-C, our work achieves mean errors of 60.12%, 56.88%, and 54.66% respectively.

Overall, our method demonstrates robust scalability across diverse models and consistently outperforms various baselines. Our results unequivocally establish the superiority of our approach, showcasing its dominance regardless of the pre-trained parameters of the source model.